

# Learned Dynamics of Electrothermally-Actuated Soft Robot Limbs Using LSTM Neural Networks

Rohan K. Mehta<sup>1</sup>, Andrew P. Sabelhaus<sup>1</sup>, Carmel Majidi<sup>1</sup>

**Abstract**—Modeling the dynamics of soft robot limbs with electrothermal actuators is generally challenging due to thermal and mechanical hysteresis and the complex physical interactions that can arise during robot operation. This article proposes a neural network based on long short-term memory (LSTM) to address these challenges in actuator modeling. A planar soft limb, actuated by a pair of shape memory alloy (SMA) coils and containing embedded sensors for temperature and angular deflection, is used as a test platform. Data from this robot are used to train LSTM neural networks, using different combinations of sensor data, to model both unidirectional (one SMA) and bidirectional (both SMAs) motion. Open-loop rollout results show that the learned model is able to predict motions over extraordinarily long open-loop timescales (10 minutes) with little drift. Prediction errors are on the order of the soft deflection sensor’s accuracy, even when using only the actuator’s pulse width modulation inputs for learning. These LSTM models can be used in-situ, without extensive sensing, helping to bring soft electrothermally-actuated robots into practical application.

## I. INTRODUCTION

Some of the most compact and easy-to-design artificial muscles for soft robots are based on electrothermal actuation [1]. These actuators are typically composed of a thermally-responsive shape changing material that can be electrically stimulated with Joule heating. Examples include coiled polymers that contract when heated [2], [3], actuators containing shape memory alloy (SMAs) wire [4], and liquid crystal elastomers [5]–[8].

However, these easy-to-use designs sacrifice the easy-to-use models of other soft actuators (e.g., pneumatics) due to the their internal actuator dynamics alongside time-dependent hysteretic behaviors [9], [10]. In particular, SMA actuators with popular materials like Nitinol have dynamics that are dictated by complex interactions at the microscopic scale. Hysteresis arises in residual stress, strain, material phase, and electrical resistance [11], so first-principles models include state variables that cannot be sensed directly [12]. Therefore, most modeling of SMA and other electrothermal actuators occurs in artificial test setups with extensive sensing capabilities [10], [11], [13]. Bringing these electrothermal actuators into practical application, such as untethered soft robotics [14], will require accurate models that can operate within significant design and sensing constraints.

This work was supported by an Intelligence Community Postdoctoral Research Fellowship through the Oak Ridge Institute for Science and Education and the National Science Foundation (NSF) National Robotics Initiative (Award: 1830362).

<sup>1</sup>R. Mehta, A.P. Sabelhaus, and C. Majidi are with the Department of Mechanical Engineering, Carnegie Mellon University, Pittsburgh PA, USA. rohanmeh, asabelha, cmajidi@andrew.cmu.edu

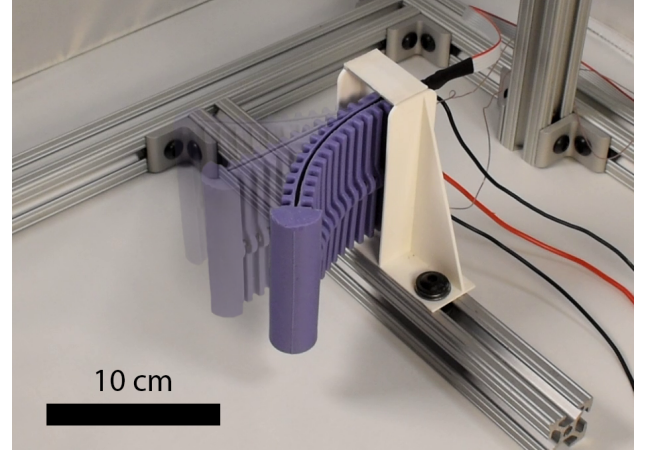


Fig. 1. This article develops a learned dynamic model of a soft, planar, electrothermally-actuated shape memory alloy (SMA) robot limb [15] using short-term memory (LSTM) neural networks. Our model can predict the limb’s deflection angle over long periods of time using combinations of power input and temperature measurements.

This work demonstrates the use of a learned model to bridge the gap between sensing capabilities and accurate dynamics predictions for a soft electrothermally actuated robot limb. The limb (Fig. 1) is powered by antagonistic pair of SMA coils and contains SMA-mounted thermocouples, as well as a dielectric elastomer bend sensor embedded within a soft silicone rubber. As motivated by recent work in other electrothermal actuators [16], we employ a long short-term memory (LSTM) neural network to learn a mapping from sensor inputs, over time, to the total bending angle of the limb (Fig. 2(A)). Our limb, using the same design as in [15], uses the embedded bend sensor and thermocouple to track the bending angle and temperature of the SMA wires respectively (Fig. 2(B)), and uses pulse-width-modulation (PWM) to apply electrical power. We collect a large dataset of motions, train LSTM networks for different combinations of PWM and temperature data, and validate our model using open-loop simulations (Fig. 1(C)). For comparison, we perform a least-squares fit on the same data, as was used in [15], and show that our LSTM network makes predictions possible using PWM duty cycles only. Our validation shows close alignment with hardware data when measurements from all of the sensors are included.

This article focuses on the modeling of our limb, in-situ, with no external sensing, analyzing the effects of different sensor data as well as different motions on learned predictions. In comparison, state-of-the-art hysteresis modeling in electrothermal actuators focuses primarily on a single type

of motion with a fixed set of external sensors [9], [10], [16]. Since many untethered SMA-actuated soft robots do not include thermal sensing [14] due to design challenges [17], we train networks both with and without that data and quantify the prediction quality that is possible given different sensors. This work improves on the approach from [18], which demonstrated the need for explicitly addressing hysteresis.

### A. Background

Prior work in soft and electrothermally-actuated robot motion has generally eschewed extensive dynamics modeling in favor of feedback control, intended to compensate for modeling errors. Feedback has been used for soft electrothermal and shape-memory actuators, but when performed with embedded sensing only, has been limited to model-free approaches [19]–[21]. However, many benefits to modeling exist in the context of motion generation, including a-priori trajectory optimization [15]. Our recent work in [15] also suggests that unloaded angular deflection predictions, as contributed by this article, can be treated as a “torque” to a robot manipulator dynamics model for loaded limb dynamics.

### B. Study Overview

This work makes the following contributions:

- 1) An open-source approach for learning dynamics models of soft electrothermally-actuated robot limbs that can predict motions given only PWM duty cycle,
- 2) A quantification of model improvement with additional sensor data (temperature), and
- 3) Open-loop rollout simulations of the robot limb, showing low error RMSE =  $5.350^\circ$  and no significant drift over very long horizons (10 minutes or more).

Combined, our results demonstrate that this type of robot can be constructed to achieve precise predictions of motion without the need for extensive sensing. Results also demonstrate noticeable improvements of predictions under bidirectional bending, with two active SMAs, in comparison to unidirectional bending with only a single SMA, producing design implications.

Though our experiment employs shape memory alloy wires as electrothermal actuators, our modeling approach does not make any assumptions about the underlying actuator technology: we use only electrical power and temperature measurements. We therefore expect these results to generalize to other electrothermal actuators exhibiting the same hysteretic characteristics, e.g., [21]. In this respect, the approach here has the potential to serve as a framework for modeling a wider range of compact soft robot limb architectures that incorporate embedded sensing.

## II. HARDWARE PLATFORM

This article considers a single robot limb, with two antagonistic shape memory alloy (SMA) actuators, designed for planar motions only. The planar design allows for simpler sensing, and isolates motions for the purpose of algorithmic development.

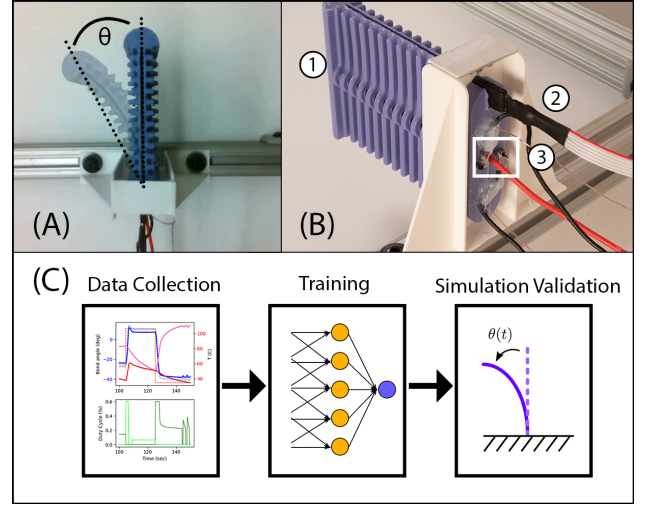


Fig. 2. Overview of our soft limb and learning procedure. (A) The soft limb has a single degree-of-freedom,  $\theta$ , for planar motion. (B) The limb is cast from bulk silicone, and is actuated by two shape-memory alloy (SMA) coils contained in a ridge along both sides of the limb (B1). Our design includes a soft bending sensor (B2) and thermocouples attached to each SMA (B3) for deflection and temperature measurements. See [15] for full details about limb construction. (C) Our procedure consists of data collection of the limb undergoing various motions, used to train our LSTM network, with the outputs validated in simulated rollouts of deflection angle.

### A. Robot Design and Fabrication

As discussed in [15], which originally presented this platform, our limb is derived from prior work on a legged soft robot [14] with the intent to eventually be employed in an untethered mobile robot. The limb itself is cast from bulk silicone rubber (Smooth-On Smooth-Sil 945). Two SMA coils extend along the length of each side of the limb (Fig. 2(B1)), made from a nickel-titanium alloy (Dynalloy Flexinol, 0.020” wire diameter). The SMA coils are crimped to stranded wire, connected to a circuit via N-channel power MOSFETs, each of which are controlled with a pulse-width modulation (PWM) voltage signal from a microcontroller. Two thermocouples (type K, 30AWG, Omega Engineering) were bonded to the SMA wires just beyond the site of the crimp using thermally conductive epoxy (MG 8329TCF), and were attached to a digital thermocouple amplifier (MAX31855). A capacitive bend sensor (Bendlabs, Inc.) is inserted into a groove in the limb (Fig. 2(B2)). Both sensors communicated with the microcontroller, which transmitted data back to a desktop computer.

### B. Robot State Space

Electrothermally-actuated robot limbs, such as that in this article, have internal state corresponding to both actuator dynamics and body dynamics. Actuator dynamics are principally governed by temperature and the temperature response given a particular amount of electrical power. Body dynamics arise from applied actuator stress.

In lieu of first-principles models that demand access to many internal states, we employ available sensor data as the inputs to our predictor. We consider four different usage

scenarios: either one SMA (unidirectional) or both antagonistic SMAs (bidirectional) actuation, and with or without temperature data. This allows us to determine the relative importance of temperature sensing, which, as with any added sensor element, represents an additional challenge in robot hardware design. The sensor input vector for the dynamics model of our soft electrothermal SMA-powered limb is denoted  $v_k(t) \in \mathbb{R}^n$ , where  $n$  varies with our inclusion of either of the two actuators and/or temperature measurements, and  $k$  denotes the particular combination of inputs:

$$v_1(t) = [u_A(t)] \quad (1)$$

$$v_2(t) = [u_A(t) \quad T_A(t)] \quad (2)$$

$$v_3(t) = [u_A(t) \quad u_B(t)] \quad (3)$$

$$v_4(t) = [u_A(t) \quad T_A(t) \quad u_B(t) \quad T_B(t)], \quad (4)$$

where  $u_j$  and  $T_j$  refer to the PWM duty cycle input and measured temperature of either SMA wire,  $j \in [A, B]$ .

### C. Data Collection Procedure

To generate the data for each of the above input spaces, two series of experiments were performed:

- 1) One single SMA was actuated, causing unidirectional counterclockwise bending (+ $\theta$  direction).
- 2) Both SMAs were used to achieve bidirectional bending (both + $\theta$  and - $\theta$  directions).

To collect this data in a realistic application, we applied a simple controller to the limb to hold different setpoint angles as a form of “motor babbling.” Setpoints of  $\bar{\theta}$  were sampled from a uniform distribution of  $[0^\circ, 45^\circ]$  for  $v_{1,2}$  and  $[-45^\circ, 45^\circ]$  for  $v_{3,4}$ , with hold times also sampled from a uniform distribution of  $[1, 30]$  sec. We used PI control for regulation, of the form  $u = K_p e + \sum_t e \Delta t$ , where  $e = (\bar{\theta} - \theta)$ . Constants were tuned by hand to be  $K_p = 0.06$  and  $K_I = 1e^{-5}$ . The result was then saturated to  $u \in [-1, 1]$  and mapped to PWM duty cycles as  $u^+ \mapsto u_A$ ,  $u^- \mapsto -u_B$ . This procedure was performed for approximately 6 hours of data, though only 30 minutes was used for training. An example of states and inputs recorded during a test is shown in Fig. (3).

## III. NEURAL NETWORK ARCHITECTURE

The framework proposed in this article consists of a neural network based on long short-term memory (LSTM) to predict the bending angle of a soft limb, tested both in one-step-ahead predictions as well as open-loop rollouts.

### A. Long Short-Term Memory (LSTM) Networks

LSTMs are a recurrent neural network (RNN) commonly applied to time series applications, due to their capability of learning order-based dependence [22]. RNNs, while able to account for a short window of relevant information, typically have difficulty propagating information across long time lags. This is referred to as the vanishing gradient problem, where error recurred through the hidden layers of an RNN can decay to zero or grow unbounded. In contrast, the LSTM architecture ensures constant error flow. This allows for complex information – such as the hysteresis in stress,

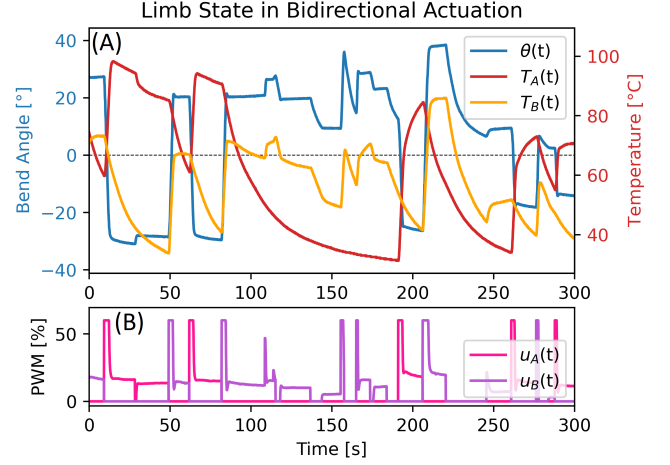


Fig. 3. Data collection test example, bidirectional. (A) Temperature of each SMA in the limb during test alongside corresponding limb angle. (B) PWM input into each SMA during test at corresponding timepoints.

strain, etc. in soft electrothermal actuator dynamics – to be carried through over a long period of time-dependence. Most importantly, LSTMs have been shown to accurately capture hysteresis in soft actuators [16] and other continuum robots [23] without the use of additional state variables.

A single LSTM node (Fig. 4(A)) takes an input  $x(t) \in \mathbb{R}^n$ , where  $n$  is the number of input features, and outputs the cell vector  $c_t \in \mathbb{R}$ , given the inputs  $x(t)$ ,  $h(t-1)$ , and  $c(t-1)$  with the following equations:

$$f(t) = \sigma(W_f x(t) + U_f h(t-1) + b_f) \quad (5)$$

$$i(t) = \sigma(W_i x(t) + U_i h(t-1) + b_i) \quad (6)$$

$$o(t) = \sigma(W_o x(t) + U_o h(t-1) + b_o) \quad (7)$$

$$\tilde{c}(t) = \tanh(W_c x(t) + U_c h(t-1) + b_c) \quad (8)$$

$$c(t) = f(t) \circ c(t-1) + i(t) \circ \tilde{c}(t) \quad (9)$$

$$h(t) = o(t) \circ \tanh(c(t)) \quad (10)$$

where  $\sigma$  is the logistic function,  $\circ$  is component-wise multiplication, and the functions  $f(\cdot), i(\cdot), o(\cdot) : \mathbb{R} \mapsto \mathbb{R}$  represent the forget gate, input gate, and output gate of the LSTM node, respectively.  $W_{f,i,o,c} \in \mathbb{R}^{h \times n}$ ,  $U_{f,i,o,c} \in \mathbb{R}^{h \times h}$ , and  $b_{f,i,o,c} \in \mathbb{R}^h$  are the matrices containing the respective input weight, recurrent weight, and bias parameters that are learned during training of the network, where  $h$  is the number of hidden neurons.

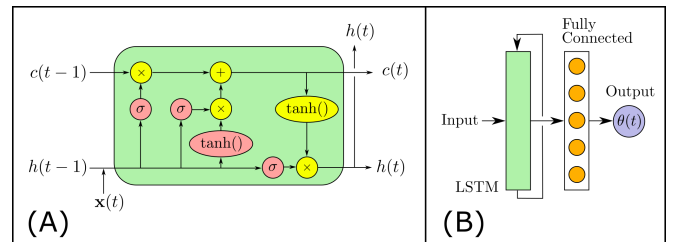


Fig. 4. Neural network architecture. (A) Visualization of an LSTM block as represented by eqns. (5-10) (B) Our network consists of an LSTM layer connected to one fully-connected neuron layer.)



### B. Network Structure and Implementation

Our neural network consists of three layers: one of LSTM nodes, one fully connected layer, and one output (Fig. 4(B)). Our model has 300 nodes in the LSTM layer and 300 nodes in the fully-connected neuron layer, which uses the ReLU activation function. The fully-connected layer leads into a single node for the output actuation state:  $\theta(t)$ . This approach is a simpler sequential network than the hierarchical LSTMs of [16], which was used for similar electrothermal twisted-coil polymer actuators.

### C. Test Setup and Training

Our network uses a time-window based representation for each configuration of sensor/actuation inputs ( $v_1$  to  $v_4$ , eqns. 1-4). Each of these is supplemented with the previous deflection angle from our onboard sensor, as per time series dynamics:

$$X_k(t) = [v_k(t) \quad v_k(t-1) \quad \theta(t-1)]$$

where  $k \in [1, 2, 3, 4]$  for each respective test using that input vector. Our predictor therefore models the dynamics function

$$\hat{\theta}(t) = g(X_k(t)). \quad (11)$$

We used the mean-squared error (MSE) loss metric below to train the model and used the root-mean-squared-error metric (RMSE) to quantify the magnitude of the difference between our predictions for point  $i$ ,  $\hat{\theta}(t)_i$ , and the ground truth data  $\theta(t)_i$ .

$$MSE = \frac{1}{n} \sum_{i=1}^n (\hat{\theta}_i(t) - \theta_i(t))^2, \quad RMSE = \sqrt{MSE} \quad (12)$$

The experimental data was split such that 67% of the time series data was selected as training data while the remaining 33% were chosen as the validation set. The bending angle data was linearly-scaled so that the maximum and minimum values lay between 1 and 0. The models were trained using the Adam optimization algorithm with a learning rate of  $10e-3$  and weight decay of 0.9. Training was performed for 20 epochs, with convergence generally observed after 10 epochs for each model. A batch size of 100 time steps was used; all other hyperparameters of the LSTM were unchanged from default values. The models implemented in Python 3.9 using the Keras API for Tensorflow running on a Google Colab notebook with a GPU-accelerated runtime environment, and has been open-sourced<sup>1</sup>.

### D. One-Step Predictions vs. Open-Loop Rollouts

Once these models were trained, we performed two experiments each to quantify their performance. First, a single-step-ahead prediction in time for each of the input vectors was performed across the test set, i.e., eqn. (11) and eqn. (12) for all datapoints  $i$  in the test set. This is done to validate that these models have been sufficiently trained to learning time-dependent information. This test is useful primarily as

a sanity check, since one-step predictions are only a basic minimum for model use (e.g. in predictive control).

Second, we employ our model in the form of its intended use: multi-step-ahead open loop rollout simulations. Starting at some initial sample in the test set, indicated as  $\tilde{\theta}(t=0)$ , our rollout recursion becomes

$$\tilde{X}_k(t) = [v_k(t) \quad v_k(t-1) \quad \tilde{\theta}(t-1)] \quad (13)$$

$$\tilde{\theta}(t) = g(\tilde{X}_k(t)), \quad (14)$$

i.e., predictions are fed back into the neural network for successive timesteps. In this case, we used a measured value from the bend sensor as our initial value, but at all future points the model has no knowledge of the true deflection angle.

Finally, these rollout predictions were compared against a simple predictor as a reference for improvement gained by using our neural network. We chose least squares regression for this task, which was performed on each test in the same manner with the same input vector  $v_k$ . It is expected that the linear regression does not capture hysteresis, and therefore will not be able to predict the nuanced behaviors of our electrothermal actuators.

## IV. RESULTS

For the one-step predictions,  $\hat{\theta}$  lies very close to the observed values  $\theta$  in all cases (Fig. 5). The best performing test in this case was Test  $k=1$  for unidirectional bending with PWM duty cycle only ( $RMSE = 0.2091^\circ$ ), while the worst performer was Test  $k=4$  for bidirectional bending with PWM duty cycle and temperature as inputs ( $RMSE = 2.613^\circ$ ). In both cases, these tests were well within the manufacturer's stated accuracy of our soft bending sensor.

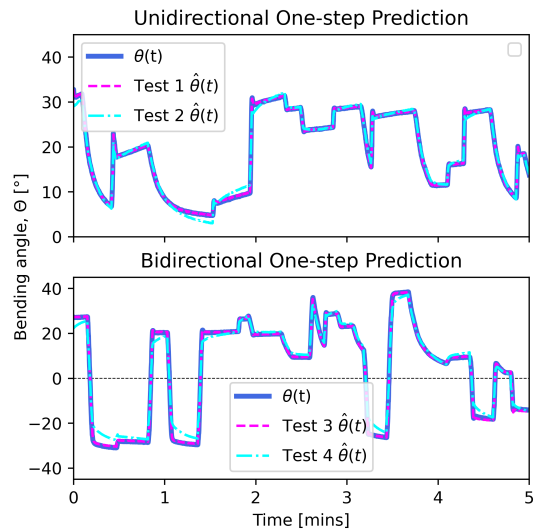


Fig. 5. Predictions of each model one time-step into the future. (A) Models trained on unidirectional data using both PWM duty cycle and temperature as inputs, i.e.,  $v_{1,2}$ . (B) Corresponding models trained on bidirectional data,  $v_{3,4}$ . Signals are virtually identical, indicating that one-step predictions are extremely accurate.

<sup>1</sup><https://github.com/rkme/memalloay>

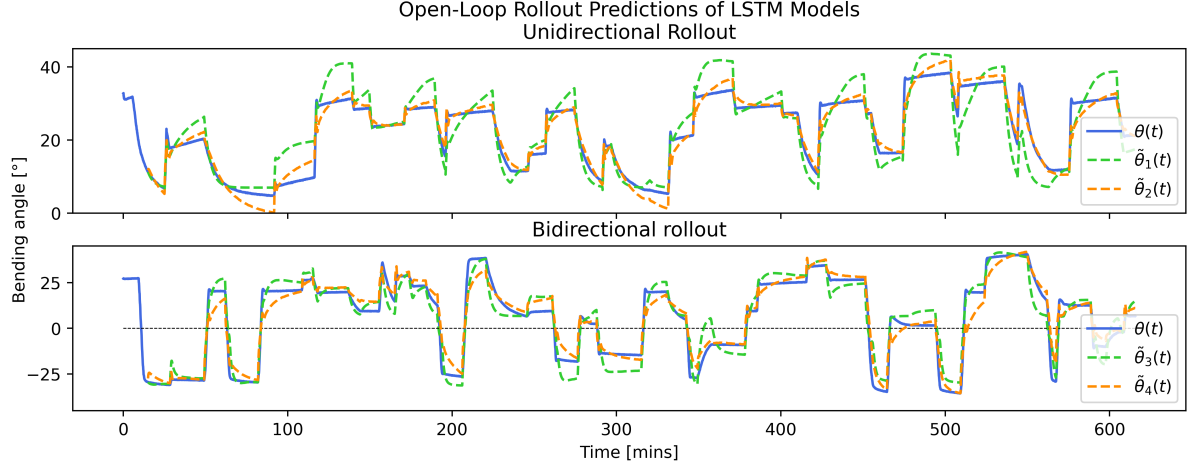


Fig. 6. Predicted rollout trajectory over 10 minutes of actuation using  $\theta(t=15s)$  as initial value. (A) Test 1 depicts rollout from the model trained only on PWM input data on a single SMA. (B) Test 2 also depicts unidirectional rollout, but uses the model trained on both PWM and temperature. (C) and (D) show the rollout for the bidirectional models trained on PWM and on PWM with temperature, respectively. All tests show extremely little drift over arbitrarily long time scales.

The results of open-loop rollout prediction across the various input spaces shows different tracking performance using different input spaces. Fig. 6 compares the predicted trajectory of the limb over time using the models trained with each input vector  $v_k$ . In general, the fewer the number of input variables that were included, the worse the performance. Ultimately, Test 4 performed the best of all the cases ( $RMSE = 5.350^\circ$ ), while Test 1 performed worst ( $RMSE = 6.296^\circ$ ). It is visually clear from Fig. (6) that the bidirectional tests outperform the unidirectional tests, and that inclusion of temperature improves prediction quality. However, all results demonstrate a usable model depending on the circumstance.

Our model also shows performance improvements over the naive least-squares fits. Using PWM-only tests, least-squares predictions are effectively noise, whereas our model shows reasonably small error in this case (Table I). This is expected, since the LSTM network captures internal state. Fits using temperature are lower error, primarily because temperature correlates reasonably well with bending angle.

However, the least-squares fit performance metric is artificially improved due to the density of our data. Fig. (7) shows the least-squares fit for the unidirectional PWM-with-temperature test ( $v_2$ ). Since our SMAs spend more time cooling down than heating, the dataset contains more cooling points. The least-squares fit is biased toward this region, and provides a very poor prediction during heating, which is of higher importance for modeling and control. In comparison, our LSTM neural network model attempts to account for hysteresis behavior during heating.

TABLE I

COMPARISON OF RMSE OF LEAST SQUARES FIT VS. LEARNED MODEL ROLLOUT, BIDIRECTIONAL MOTIONS

Test Case	Least Squares RMSE	LSTM Rollout RMSE
Test 3 ( $u_j$ only)	$19.01^\circ$	$6.151^\circ$
Test 4 ( $u_j$ and $T_j$ )	$6.372^\circ$	$5.350^\circ$

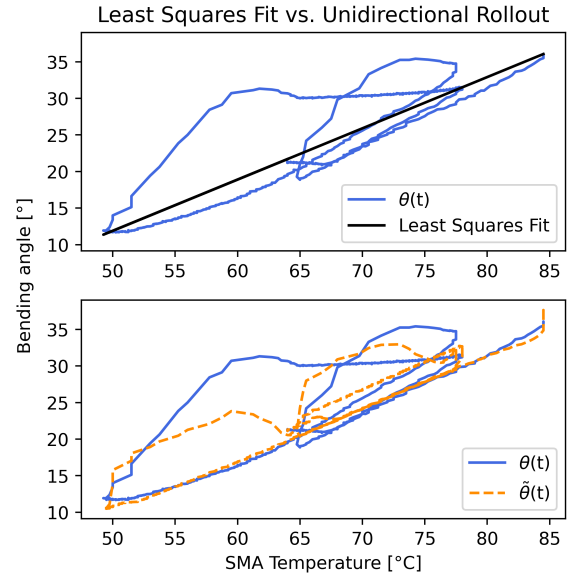


Fig. 7. Demonstration of improved hysteresis characterization predicted from  $\hat{\theta}$  rollout prediction on unidirectional bending trained on  $u_1$  and  $T_1$ . The LSTM captures some hysteric effects over time whereas a naive least-squares comparison does not.

## V. DISCUSSION AND CONCLUSION

These learned LSTM-based neural network dynamics models appear to capture the core physics that govern soft, electrothermally-actuated limbs. Single-step-ahead predictions validate that our model sufficiently learned the importance of time-dependent behaviors, and open-loop rollouts produce low-drift predictions over extremely long time periods (i.e.  $\sim 10$  minutes). In the scenario of the most amount of data – bidirectional bending with temperature included – predictions are of low error in all regions of the state space. The RSME error in the resultant predictions were on the same order of our sensor accuracy. Predictions were performed  $2.4\times$  faster than real-time, which is promising for

feedback control applications. However, improvements can still be made to reduce error.

When training on only the PWM duty cycles, particularly in the unidirectional case (Fig. 6(A)), our model consistently overshoots the expected deflection angle. This could be attributed to less data available, due to fewer inputs, or more hysteretic behaviors with single-SMA motions: the only restoring force is due to the soft silicone. However, in the bidirectional case, rollouts using PWM inputs only show surprisingly accurate predictions. As a result, it may be possible to model these electrothermally-actuated soft robot limbs without temperature sensing. Mechanical designs for untethered soft thermal actuator robots can therefore be made simpler while still maintaining our capability for dynamics predictions. Possible future work includes experiments with more neural network layers and architectures, as well as tuning of hyperparameters.

Inclusion of temperature is observed to reduce or eliminate overshoot in the predictions. The RMSE error improvement is small over the course of the entire test set in the bidirectional case (approximately 13% lower error); however, visual inspection of Fig. (6) shows qualitative improvements.

In all cases, the response in predicted angle has a slight time delay in comparison to the test data. Many of the results in Fig. (6) do not appear to capture sharp increases in bending angle. This may be due to the added thermal mass from the epoxy joint at the site of thermocouple attachment, which could be addressed using the method from [15].

The tests above utilize ground-truth temperature measurements during open-loop rollouts. These would not be available during online prediction scenarios, as would be the case for feedback control. However, we consider these tests to be valid, since prior work has shown that temperature of SMA wires can be predicted reasonably well from Joule heating models [15] and that LSTM networks may also be able to predict temperature itself [16]. A possible direction for future work is therefore predicting temperature alongside bending angle. Our temperature-free models, which do not have this drawback, can still be used for true open-loop predictions.

This work contributes an approach for dynamics predictions of electrothermally-actuated soft robot limbs that can be used with minimal sensor data, in-situ, with accuracy on the order of soft sensing capabilities. The model therefore bridges a crucial gap between hysteretic, difficult-to-model actuators and practical use in soft robotics applications. Future work can incorporate these models as part of predictive control algorithms for positioning of these soft limbs. These models also have the potential to be implemented into soft robotic limbs for untethered locomotion.

## REFERENCES

- [1] S. I. Rich, R. J. Wood, and C. Majidi, "Untethered soft robotics," *Nature Electronics*, vol. 1, no. 2, Feb. 2018.
- [2] C. S. Haines, M. D. Lima, N. Li, G. M. Spinks, J. Foroughi, J. D. Madden, S. H. Kim, S. Fang, M. J. De Andrade, F. Göktepe, *et al.*, "Artificial muscles from fishing line and sewing thread," *Science*, vol. 343, no. 6173, pp. 868–872, 2014.
- [3] B. Pawlowski, J. Sun, J. Xu, Y. Liu, and J. Zhao, "Modeling of Soft Robots Actuated by Twisted-and-Coiled Actuators," *IEEE/ASME Transactions on Mechatronics*, vol. 24, no. 1, Feb. 2019.
- [4] H. Rodrigue, W. Wang, M.-W. Han, T. J. Kim, and S.-H. Ahn, "An Overview of Shape Memory Alloy-Coupled Actuators and Robots," *Soft Robotics*, vol. 4, no. 1, Mar. 2017.
- [5] C. Yuan, D. J. Roach, C. K. Dunn, Q. Mu, X. Kuang, C. M. Yakacki, T. J. Wang, K. Yu, and H. Jerry Qi, "3D printed reversible shape changing soft actuators assisted by liquid crystal elastomers," *Soft Matter*, vol. 13, no. 33, 2017.
- [6] Q. He, Z. Wang, Y. Wang, A. Minori, M. T. Tolley, and S. Cai, "Electrically controlled liquid crystal elastomer-based soft tubular actuator with multimodal actuation," *Science Advances*, vol. 5, no. 10, Oct. 2019.
- [7] M. J. Ford, C. P. Ambulo, T. A. Kent, E. J. Markvicka, C. Pan, J. Malen, T. H. Ware, and C. Majidi, "A multifunctional shape-morphing elastomer with liquid metal inclusions," *Proceedings of the National Academy of Sciences*, vol. 116, no. 43, Oct. 2019.
- [8] T. A. Kent, M. J. Ford, E. J. Markvicka, and C. Majidi, "Soft actuators using liquid crystal elastomers with encapsulated liquid metal joule heaters," *Multifunctional Materials*, vol. 3, no. 2, June 2020.
- [9] C. Xiang, H. Yang, Z. Sun, B. Xue, L. Hao, M. D. A. Rahoman, and S. Davis, "The design, hysteresis modeling and control of a novel SMA-fishing-line actuator," *Smart Materials and Structures*, vol. 26, no. 3, Feb. 2017.
- [10] J. Z. Ge, L. Chang, and N. O. Pérez-Arancibia, "Preisach-model-based position control of a shape-memory alloy linear actuator in the presence of time-varying stress," *Mechatronics*, vol. 73, p. 102452, Feb. 2021.
- [11] M. Zakerzadeh, H. Salehi, and H. Sayyaadi, "Modeling of a Nonlinear Euler-Bernoulli Flexible Beam Actuated by Two Active Shape Memory Alloy Actuators," *Journal of Intelligent Material Systems and Structures*, vol. 22, no. 11, July 2011.
- [12] S. Majima, K. Kodama, and T. Hasegawa, "Modeling of shape memory alloy actuator and tracking control system with the model," *IEEE Transactions on Control Systems Technology*, vol. 9, no. 1, pp. 54–59, 2001.
- [13] J. Lee, M. Jin, and K. K. Ahn, "Precise tracking control of shape memory alloy actuator systems using hyperbolic tangential sliding mode control with time delay estimation," *Mechatronics*, vol. 23, no. 3, pp. 310–317, Apr. 2013.
- [14] Z. J. Patterson, A. P. Sabelhaus, K. Chin, T. Hellebrekers, and C. Majidi, "An Untethered Brittle Star-Inspired Soft Robot for Closed-Loop Underwater Locomotion," in *2020 IEEE/RSJ International Conference on Intelligent Robots and Systems (IROS)*, Oct. 2020, pp. 8758–8764.
- [15] A. Wertz, A. P. Sabelhaus, and C. Majidi, "Trajectory Optimization for Thermally-Actuated Soft Planar Robot Limbs," *arXiv:2110.09474 [cs]*, Oct. 2021, arXiv: 2110.09474.
- [16] A. T. Luong, H. Moon, H. R. Choi, J. C. Koo, S. Seo, K. Kim, J. Jeon, C. Park, and M. Doh, "Long short term memory model based position-stiffness control of antagonistically driven twisted-coiled polymer actuators using model predictive control," *IEEE Robotics and Automation Letters*, pp. 1–1, 2021.
- [17] C. Majidi, "Soft-matter engineering for soft robotics," *Advanced Materials Technologies*, vol. 4, no. 2, p. 1800477, 2019.
- [18] A. P. Sabelhaus and C. Majidi, "Gaussian process dynamics models for soft robots with shape memory actuators," in *2021 IEEE 4th International Conference on Soft Robotics (RoboSoft)*. IEEE, 2021, pp. 191–198.
- [19] N. Ma, G. Song, and H.-J. Lee, "Position control of shape memory alloy actuators with internal electrical resistance feedback using neural networks," *Smart Materials and Structures*, vol. 13, no. 4, June 2004.
- [20] M. H. Elahinia and H. Ashrafioun, "Nonlinear Control of a Shape Memory Alloy Actuated Manipulator," *Journal of Vibration and Acoustics*, vol. 124, no. 4, pp. 566–575, Oct. 2002.
- [21] A. Kotikian, J. M. Morales, A. Lu, J. Mueller, Z. S. Davidson, J. W. Boley, and J. A. Lewis, "Innervated, Self-Sensing Liquid Crystal Elastomer Actuators with Closed Loop Control," *Advanced Materials*, vol. 33, no. 27, p. 2101814, 2021.
- [22] S. Hochreiter and J. Schmidhuber, "Long short-term memory," *Neural computation*, vol. 9, no. 8, pp. 1735–1780, 1997.
- [23] Q. Zhao, J. Lai, K. Huang, X. Hu, and H. K. Chu, "Shape estimation and control of a soft continuum robot under external payloads," *IEEE/ASME Transactions on Mechatronics*, 2021.